Bioorganic & Medicinal Chemistry 18 (2010) 7065–7077

Contents lists available at ScienceDirect

Bioorganic & Medicinal Chemistry

journal homepage: www.elsevier.com/locate/bmc

Structure–activity relationships in 1,4-benzodioxan-related compounds. 10. Novel α_1-adrenoreceptor antagonists related to openphendioxan: Synthesis, biological evaluation, and α_{1d} computational study ☆

Antonio Carrieri [a,*], Alessandro Piergentili [b], Fabio Del Bello [b], Mario Giannella [b], Maria Pigini [b], Amedeo Leonardi [c], Francesca Fanelli [d], Wilma Quaglia [b,*]

[a] Dipartimento Farmaco-Chimico, Università di Bari, via Orabona 4, 70125 Bari, Italy
[b] Scuola di Scienze del Farmaco e dei Prodotti della Salute, Università di Camerino, via S. Agostino 1, 62032 Camerino, Italy
[c] Recordati S. p. A., Drug Discovery, via Civitali 1, 20148 Milano, Italy
[d] Istituto Dulbecco Telethon e Dipartimento di Chimica, Università di Modena & Reggio Emilia, via Campi 183, 41100 Modena, Italy

ARTICLE INFO

Article history:
Received 23 April 2010
Revised 28 July 2010
Accepted 2 August 2010
Available online 6 August 2010

Keywords:
GPCRs
α_1-Adrenoreceptor antagonists
Openphendioxan analogues
QSAR
Comparative modeling
Docking

ABSTRACT

A series of novel openphendioxan analogues were synthesized and tested at α_1-adrenoreceptor (AR) subtypes by binding and functional assays. The α_{1d}-AR binding profile was also examined by means of 2D, 3D-QSAR together with docking studies. Multiple regression analysis suggested the relevance of adequate number of heteroatoms in the whole molecule and of passive membrane diffusion to enhance α_{1d}-AR affinity. Docking simulations against a computational structural model of the biological target further proved this evidence and furnished support for chemiometric analysis, where polar, electrostatic, hydrophobic and shape effects of the ortho substituents in the phenoxy terminal, most likely governing ligand binding, helped the depiction of pharmacophore hypothesis for the examined ligands data set.

1. Introduction

Insights gained from target proteins and receptors three-dimensional structure are pivotal for successful modern drug design. The number of entries deposited at the Protein Data Bank[2] (PDB) is nowadays more than sixty thousand, with more than five thousand new structures available each year. However, compared to these valuable numbers, very few data refer to integral proteins (180 unique structures).[3] The paucity of robust information on structural assembly of transmembrane (TM) receptors holds back the discovery rate of novel compounds acting as binders to G-protein-coupled receptors (GPCRs), the target of approximately half of the top 100 drugs currently on the market. Sensational breakdowns were determined first in year 2000, when the X-ray structure of bovine rhodopsin was solved by Palczewski et al.[4] and later with the achievement of human β_1- and β_2-adrenergic[5,6] and A_{2A} adenosine receptor crystallographic data.[7] In the light of this mutated scenario, the rational design of novel molecules interacting with the adrenergic receptors turns to a more feasible effort.

The widespread expression in many human tissues and the involvement in numerous physiological processes make adrenoreceptors (ARs) highly attractive pharmacological targets for the treatment of numerous pathologies.[8] Particularly, the three subtypes belonging to the α_1-AR family (α_{1A}, α_{1B}, and α_{1D})[9] have different distribution[10] and modulate a large number of physiological functions in cardiovascular and non cardiovascular tissues. The α_{1A}-AR subtype is considered to be the main system contributing to the dynamic (phasic) component of increased bladder outlet resistance[11] and, together with the α_{1D} subtype, mediating lower urinary tract symptoms (LUTS) caused by benign prostatic hyperplasia (BPH).[12] For this reason α_1-antagonists selective for α_{1A}- and/or α_{1A}- + α_{1D}-AR subtypes with respect to the α_{1B} subtype are clinically useful in the treatment of BPH,[13] avoiding cardiovascular and orthostatic

Abbreviations: GPCR, G-protein-coupled receptor; AR, adrenoreceptor; TM, transmembrane; LUTS, lower urinary tract symptoms; BPH, benign prostatic hyperplasia; TM, transmembrane; SDM, site-directed mutagenesis; PDB, protein data bank; CHO, chinese hamster ovary; QSARs, quantitative structure–activity relationships; [^3H]8-OH-DPAT, 8-hydroxy-2-(di-*n*-propylamino)tetralin; SAR, structure–activity relationships; SAFIR, structure–affinity relationships; QPlogBB, predicted blood–brain barrier partition coefficient; K_i, inhibition or dissociation constant; K_b, dissociation constant; MRA, multiple regression analysis; PLS, partial least squares; MIF, molecular interaction field.

☆ See Ref. 1.

* Corresponding authors. Tel.: +39 0805442638; fax: +39 0805442724 (A.C.); tel.: +39 0737402237; fax: +39 0737637345 (W.Q.).
E-mail addresses: carrieri@farmchim.uniba.it (A. Carrieri), wilma.quaglia@unicam.it (W. Quaglia).

0968-0896/$ - see front matter © 2010 Elsevier Ltd. All rights reserved.
doi:10.1016/j.bmc.2010.08.002

hypotensive side effects.[14] The observation that the α_{1B}-AR subtype controls locomotor and rewarding effects of psychostimulants and opiates suggests the use of antagonists targeting this subtype in the treatment of drug abuse.[15] Moreover, the role of α_1-ARs in the mitogenic effect of catecholamines on prostate growth has been demonstrated[16] and recent studies have highlighted the efficacy of α_{1D}- and α_{1B}-AR antagonists in the modulation of apoptosis and cell proliferation.[17] Unfortunately, the high homology among the TM domains of the three α_1-AR subtypes limits the availability of ligands with adequate subtype selectivity. Indeed, site-directed mutagenesis (SDM) studies reported that two phenylalanines in TM7 domain (Phe7.35 and Phe7.39 according to the Ballesteros and Weinstein numbering)[18] are highly conserved among all the three α_1-AR subtypes[19] and are involved in high-affinity binding for many α_1-AR antagonists, among which [2-(2,6-dimethoxyphenoxy)-ethyl][(2,3-dihydro-1,4-benzodioxin-2-yl)methyl]-amine (WB4101) (Fig. 1).[20] Some of us have previously demonstrated that the insertion of a trans phenyl (phendioxan) or *p*-tolyl (mephendioxan) moiety in position 3 of WB4101 increased affinity and selectivity for α_{1A}-ARs, whereas the replacement of the oxygen atom in position 4 with a phenylmethine group afforded an α_{1D} selective antagonist.[20] α_{1D} selectivity was also obtained by opening the dioxane ring of phendioxan affording openphendioxan (**1**)[21] (Fig. 1). Moreover, we also demonstrated that the introduction of substituents, having all the possible combinations of σ and π parameters in the benzyloxy portion of **1**, did not significantly affect its already high α_{1D}-AR affinity.[17]

However, since it is known that aromaticity/hydrophobicity might play an important role in the antagonist receptor interaction and subtype discrimination,[19] in the present study, taken **1** as lead compound, some chemical modifications were performed in its 2,6-dimethoxyphenoxy portion. The novel compounds were obtained by replacing the oxygen atom of the bridge spacing the basic centre and the 2,6-dimethoxyphenyl ring with its S or CH_2 bioisosteres or an SO function (**2**–**4**), by removing one or both 2,6-dimethoxy substituents, or by replacing one or both of them with groups of different physicochemical (electronic and steric) properties (**5**–**14**) (Fig. 1). The biological profiles of the novel compounds were assessed by binding assays at human cloned α_1-AR subtypes and 5-HT_{1A} receptors, expressed in Chinese hamster ovary (CHO) and HeLa cell membranes, respectively, and by functional experiments in isolated rat vas deferens (α_{1A}), spleen (α_{1B}), and aorta (α_{1D}). Afterwards, computational quantitative structure–activity relationships (QSARs), homology modeling, and docking studies were conducted to highlight the influence of the ortho substitution in the terminal phenyl ring of the basic chain on α_{1d}-AR affinities. The α_1-AR antagonist WB4101[20] was included in this investigation for useful comparison.

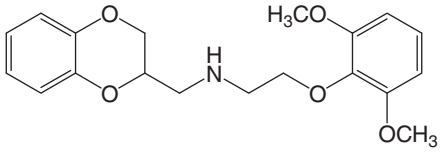

WB4101

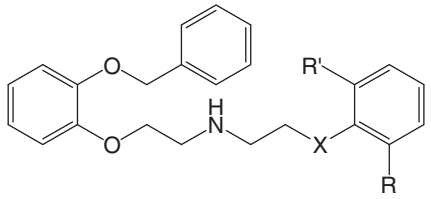

1: X=O, R=R'=OCH_3
2: X=S, R=R'=OCH_3
3: X=CH_2, R=R'=OCH_3
4: X=SO, R=R'=OCH_3
5: X=O, R=R'=OC_2H_5
6: X=O, R=OCH_3, R'=NO_2
7: X=O, R=OCH_3, R'=Cl
8: X=O, R=OCH_3, R'=CH_3
9: X=O, R=OC_2H_5, R'=H
10: X=O, R=OCH_3, R'=H
11: X=O, R=R'=Cl
12: X=O, R=R'=CH_3
13: X=O, R=R'=OH
14: X=O, R=R'=H

Figure 1. Chemical structures of WB4101, openphendioxan (**1**), and the novel compounds **2**–**14**.

2. Chemistry

The novel compounds **2**–**14** were synthesized according to the methods reported in Schemes 1 and 2. Alkylation of 2,6-dimethoxybenzenethiol,[22] 2,6-diethoxyphenol,[23] and 2-(benzyloxy)phenol with 2-chloroacetamide afforded the intermediate amides **15**–**17**, respectively, which were reduced with borane–dimethyl sulfide complex in dry THF to give the corresponding amines **18**–**20**. Amidation of **18**, **19**, and other proper substituted phenoxyethanamines, commercially available or prepared following the procedure reported in the literature,[24] with 2-[2-(benzyloxy)phenoxy]acetic acid[21] in the presence of Et_3N and EtOCOCl furnished amides **21**–**28**, whose reduction with borane–dimethyl sulfide complex in dry THF afforded the final compounds **2**, **5**, **7**, **9**–**12**, and **14**. Oxidation of **2** with H_2O_2 in acetic acid gave compound **4** (Scheme 1). Similarly, compounds **3**, **6**, **8**, and **13** were synthesized, according to Scheme 2, by amidation of **20** with the proper disubstituted phenoxyacetic acid and subsequent reduction of the amides **29**–**32** with borane–dimethyl sulfide complex in dry THF. 3-(2,6-Dimethoxyphenyl)propanoic acid, 2-(2-methoxy-6-nitrophenoxy)acetic acid, and 2-(2-methoxy-6-methylphenoxy)acetic acid were prepared according to the literature.[25–27] In the case of 2-(2,6-bis(methoxymethoxy)phenoxy)acetic acid (**35**), the procedure reported in Scheme 3 was followed. Thus, lithiation of 1,3-bis(methoxymethoxy)benzene[28] with *n*-BuLi, followed by boronation–oxidation with $B(OMe_3)_3$ and oxone in aqueous acetone–$NaHCO_3$, afforded the phenol **33**, whose treatment with methyl chloroacetate gave **34**, which was hydrolyzed to the corresponding acid **35**.

3. Results and discussion

The affinity constants, expressed as pK_i, of compounds **2**–**14** were evaluated by radio-receptor binding assays using **1** and WB4101 as reference compounds. [^3H]Prazosin was used to label cloned human α_1-ARs expressed in CHO cells.[29] Furthermore, [^3H]8-hydroxy-2-(di-*n*-propylamino)tetralin ([^3H]8-OH-DPAT) was used to label cloned human 5-HT_{1A} receptors expressed in HeLa cells.[30,31]

The pharmacological profile of compounds **2**–**14** was further determined at α_1-ARs on different isolated tissues using **1** and WB4101 as reference compounds. α_1-AR subtypes blocking activity, expressed as pK_b, was assessed by antagonism of (−)-noradrenaline-induced contraction of rat prostatic vas deferens (α_{1A})[32] or thoracic aorta (α_{1D})[33] and by antagonism of (−)-phenylephrine-induced contraction of rat spleen (α_{1B}).[34]

From an analysis of the results reported in Table 1 interesting considerations emerged. All the substitutions of the oxygen atom in the bridge (**2**–**4**) induced the maintenance of high α_{1d}-affinity and preferential α_{1d}-AR subtype interaction with respect to α_{1a}- and α_{1b}-AR subtypes. However, while the bioisosteric sulfur analogue **2** showed affinity values similar to those of **1**, the replacement of the oxygen atom with a methylene group (**3**) or the oxidation of the sulfur atom to the sulfoxide function (**4**) did not

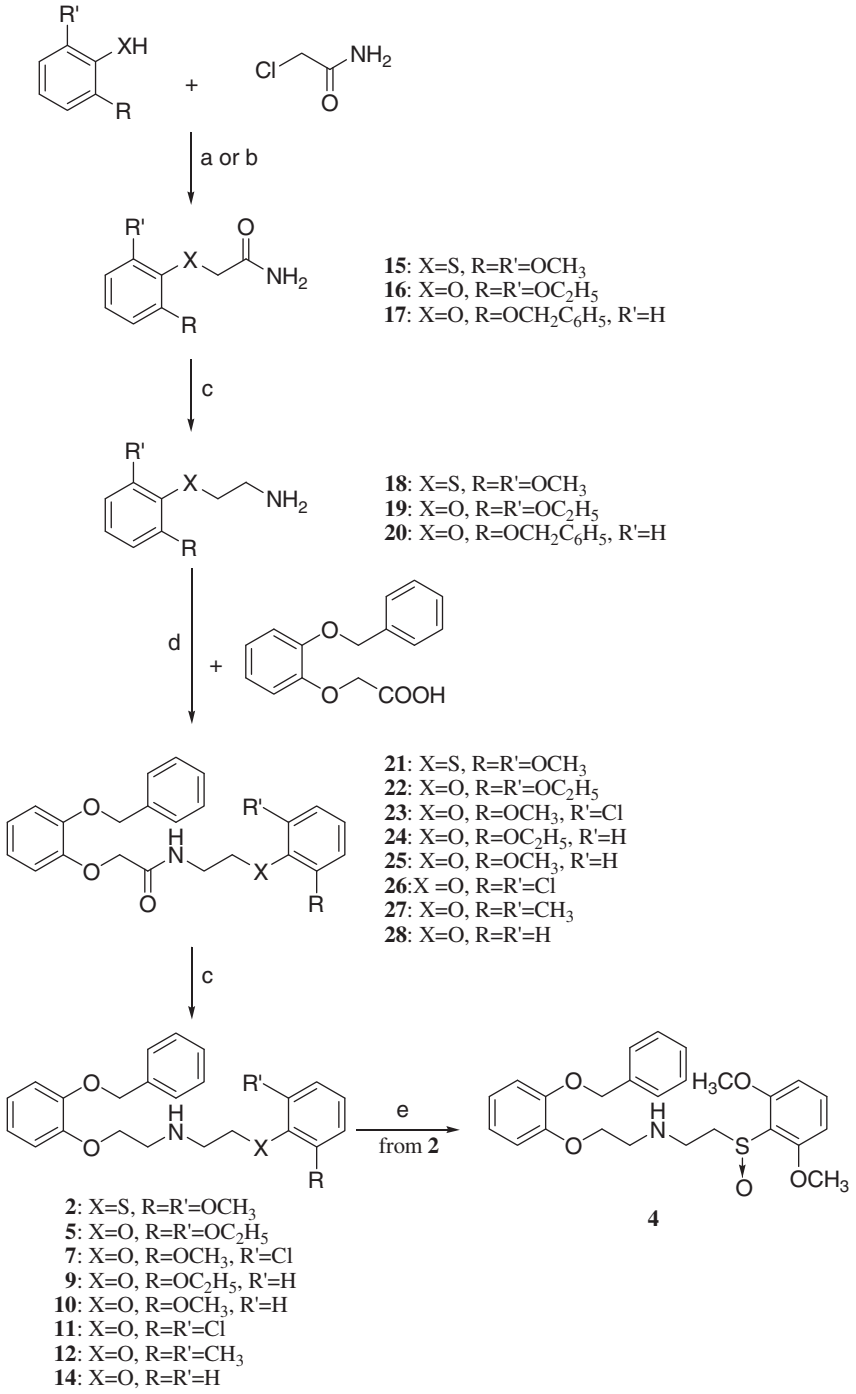

Scheme 1. Reagents: (a) Na, KI, EtOH; (b) K_2CO_3, acetone; (c) $BH_3{\cdot}Me_2S$, THF; (d) Et_3N, EtOCOCl, $CHCl_3$; (e) 30% H_2O_2, AcOH.

favourably contribute to the general α_1-AR interaction. This result, which was more and more evident considering the functional antagonist affinities, suggested that the good electronic density provided by oxygen and sulfur atoms, and not associated with a spatially defined orientation as in the case of the SO function, determined more productive interactions. The pK_b values observed in functional experiments, comparable in most cases with the pK_i affinities derived from the binding assays, highlighted for **3** and, especially, for **4** the loss of the α_{1D} selectivity. The discrepancy between functional and binding affinities meets a common justification in the different arrangement of native or cloned receptor populations.[35] In contrast, the presence of a methylene or sulfoxide moiety enhanced the 5-HT_{1A}-affinity of the lead. Removal of one or both methoxy groups (**10** and **14**, respectively) as well as their simultaneous replacement with smaller substituents such as chloro, methyl and hydroxy groups (**11**–**13**) caused a sharp decrease in both binding and functional affinities for all the α_1-AR subtypes and in α_{1d}-AR subtype selectivity. Instead, such modifications did not significantly affect the 5-HT_{1A} affinity. The 2,6-diethoxy derivative **5** showed a biological affinity profile similar to that of **1**, suggesting that the small increase of the steric bulk was tolerated. In this case the removal of one ethoxy group (**9**) reduced the affinities for α_{1b}- and α_{1d}-AR subtypes. The binding profile of derivatives **5** and **9** was not confirmed by functional data, from

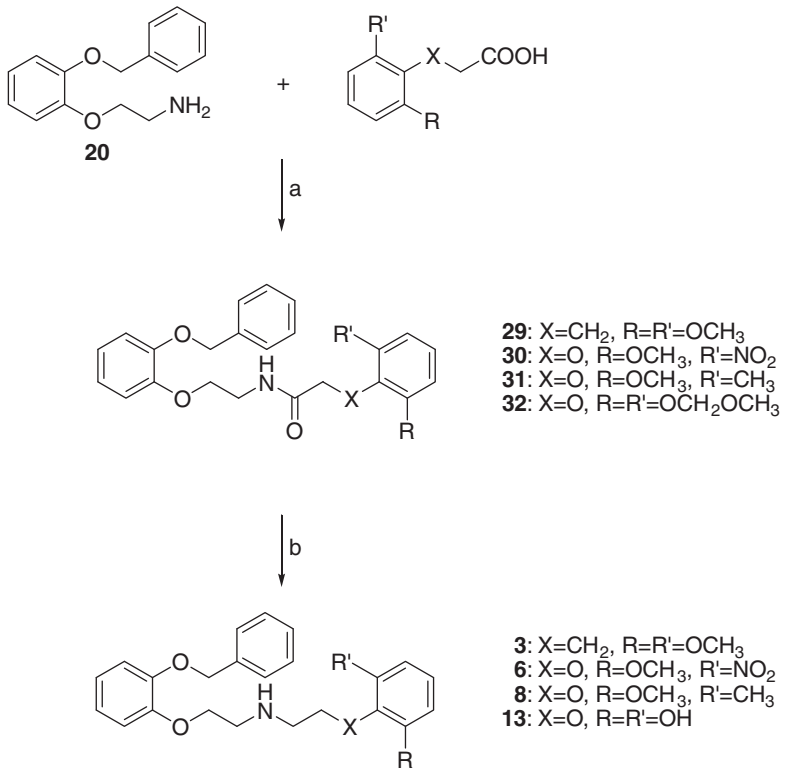

Scheme 2. Reagents: (a) Et_3N, EtOCOCl, $CHCl_3$; (b) $BH_3{\cdot}Me_2S$, THF.

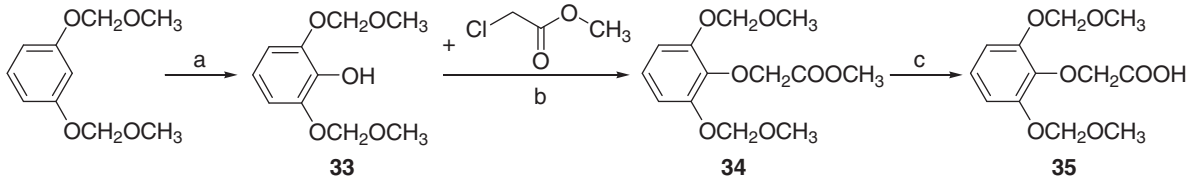

Scheme 3. Reagents: (a) *n*-BuLi, $B(OMe)_3$, oxone, THF; (b) K_2CO_3, KI, acetone; (c) 2 N NaOH.

which compound **5** showed the highest antagonist affinity and a preferential selectivity for α_{1B}-AR subtype with respect to the other subtypes. The removal of one ethoxy group (compound **9**) significantly affected only the potency at α_{1B}-AR subtype. The replacement of only one of the two methoxy groups of **1** with a nitro, chloro, or methyl substituent (**6**–**8**) was compatible with a preferential and efficient α_{1d} interaction. The observation that the derivatives **7** and **8** showed affinity values significantly higher than those of the corresponding equally disubstituted derivatives **11** and **12** suggested that, for a high α_{1d}-affinity, at least one of the two ortho substituents should be a methoxy group. Moreover, interestingly, among the novel derivatives, analogously to lead **1**, compounds **2** and **5**–**7** proved to be endowed with a significant α_{1d}-AR/5-HT_{1A} selectivity.

Classical QSARs were further applied on the highly congeneric derivatives **1** and **5**–**14** to rationalize their α_{1d}-AR affinity spectrum using a large and fresh set of molecular descriptors providing a complete level of information with different 1D and 2D indices, related not only to physicochemical, but also to topological, geometrical, quantum chemical and pharmacokinetics features of the ligand, included in the QikProp software package (see Table 2).[36]

In a first instance, taking into account affinities referred only to compounds **5**–**14** the measured affinity constants, through plausible parabolic dependence (r^2 >0.65), resulted to be nearly affected by the largeness of the substituents, as measured by QikProp volume (compound **1** was excluded most likely due to the data distribution). This evidence is supported by the significant drop of the same constants caused by the absence of any functional group in the phenoxy moiety (compound **14**). Moreover, our results agreed with previous studies[24,37] confirming the essential role of the ortho substituents with certain steric hindrance.

Afterwards we gain better and further insights into the structure–affinity relationships (SAFIR) carrying out a statistical analysis with STRIKE.[38] This modeling tool, automatically, performs multiple regression analysis to derive several QSAR equations using different properties associated to ligand structures. Among the whole set of fifty QikProp descriptors, the best and statistically most significant relationship (Eq. 1) was achieved with two independent variables, the predicted blood–brain barrier partition coefficient QPlogBB and the number of nitrogen and oxygen atoms present in the molecule #NandO. The aforementioned variables, encoding passive membrane diffusion and polarity, scored with positive coefficients, lipophilicity and hydrogen bonding capability as major determinants for the antagonist binding. It could then be suggested that molecular properties, mimicked by the parameters present in (Eq. 1), should have a relevant weight on controlling and affecting the largeness of the pK_i value and, therefore, the whole receptor binding process.

Table 1
Affinity constants, expressed as pK_i, of compounds **1**–**14** and WB4101 for human recombinant α_1-AR subtypes and 5-HT_{1A} receptor[a]. Antagonist affinities, expressed as pK_b values at α_1-ARs on isolated rat vas deferens (α_{1A}), spleen (α_{1B}), and thoracic aorta (α_{1D})[b]

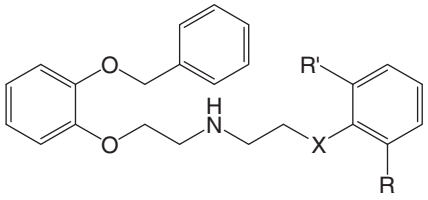

Compd	R	R'	X	pK_i[a] human cloned receptors				pK_b[b]		
				α_{1a}	α_{1b}	α_{1d}	5-HT_{1A}	α_{1A}	α_{1B}	α_{1D}
1	OCH_3	OCH_3	O	9.33	9.27	10.17	7.93	8.39 ± 0.18	8.30 ± 0.15	9.37 ± 0.15
2	OCH_3	OCH_3	S	8.50	9.30	9.75	7.80	8.74 ± 0.10	8.57 ± 0.09	9.47 ± 0.11
3	OCH_3	OCH_3	CH_2	8.01	8.16	8.92	8.60	7.80 ± 0.04	7.34 ± 0.18	8.12 ± 0.05
4	OCH_3	OCH_3	SO	7.70	7.80	8.56	8.50	7.95 ± 0.05	7.65 ± 0.08	7.49 ± 0.03
5	OC_2H_5	OC_2H_5	O	8.50	9.10	9.41	7.50	7.92 ± 0.04	8.57 ± 0.03	8.03 ± 0.17
6	OCH_3	NO_2	O	8.95	8.30	9.29	7.80	8.41 ± 0.04	8.19 ± 0.05	8.92 ± 0.09
7	OCH_3	Cl	O	8.60	8.10	9.13	7.50	8.16 ± 0.05	7.84 ± 0.07	8.74 ± 0.02
8	OCH_3	CH_3	O	8.60	8.30	9.04	8.40	8.35 ± 0.02	7.91 ± 0.09	8.36 ± 0.13
9	OC_2H_5	H	O	8.70	7.90	8.43	8.30	8.03 ± 0.04	7.94 ± 0.04	8.35 ± 0.07
10	OCH_3	H	O	8.50	7.70	8.40	8.60	7.95 ± 0.07	7.89 ± 0.14	8.08 ± 0.06
11	Cl	Cl	O	8.20	7.10	8.15	7.50	6.57 ± 0.13	7.75 ± 0.03	8.02 ± 0.02
12	CH_3	CH_3	O	8.10	7.0	7.85	7.80	7.33 ± 0.14	7.78 ± 0.10	7.59 ± 0.03
13	OH	OH	O	8.30	7.0	7.82	7.90	7.44 ± 0.07	7.02 ± 0.01	7.44 ± 0.03
14	H	H	O	8.0	7.0	7.75	8.10	7.65 ± 0.10	7.74 ± 0.11	7.32 ± 0.03
WB4101				9.37	8.0	9.29	8.68	9.51 ± 0.06	8.16 ± 0.09	8.80 ± 0.12

[a] Equilibrium dissociation constants (K_i) were derived from IC_{50} values using the Cheng–Prusoff equation.[48] The affinity estimates were derived from displacement of [^3H]prazosin and [^3H]-8-hydroxy-2-(di-*n*-propylamino)tetralin binding for α_1-ARs and 5-HT_{1A} receptor, respectively. Each experiment was performed in triplicate. K_i values were from two to three experiments, which agreed within ±20%.
[b] pK_b values were calculated according to van Rossum[46] in the range 0.01–10 μM. Each concentration [B] of antagonist was tested four times.

Table 2
QikProp molecular descriptors of compounds **1** and **5**–**14**

Compd	V[a]	QPlogBB[b]	#NandO[c]
1	146.61	0.135	6
5	273.91	0.015	6
6	139.21	−0.810	8
7	107.57	0.312	5
8	161.62	0.209	5
9	147.54	0.101	5
10	75.24	0.165	5
11	77.67	0.503	4
12	102.65	0.216	4
13	37.75	−0.819	6
14	0.00	0.227	4

[a] Measured as difference between the solvent accessible volume in cubic Å of substituted and unsubstituted compounds using a probe with a 1.4 Å radius.
[b] Predicted blood–brain partitioning.
[c] Number of nitrogen and oxygen atoms.

$$\begin{aligned} p\mathit{K}_i &= 2.226(\pm 0.360)\mathrm{QPlogBB} \\ &\quad + 1.033(\pm 0.1307)\#\mathrm{NandO} + 3.18(\pm 0.701) \qquad (1) \\ n &= 11;\ r^2 = 0.887;\ s = 0.296;\ F = 31.30 \end{aligned}$$

To go further on this topic, WB4101 and derivatives **1**–**14** were docked to a computational model of the α_{1d}-AR, realized by comparative modeling by using the X-ray structure of the β_2-AR as a template. The aim was to sketch a more detailed framework of α_{1d}-AR ligands binding process and to probe, at three-dimensional level, the hypothesis formulated by the 2D-QSAR study about the role of ortho substituents as major molecular determinants for α_{1d}-AR antagonism. Flexible docking furnished valuable indications on the binding topology characterizing openphendioxan analogues and helped to rationalize the different experimentally determined receptor affinities, suggesting that slightly hindered and hydrogen bonding acceptor groups might properly orient the antagonist scaffold, favoring and stabilizing the different interactions essential to increase affinity.

This assumption can be perceived in details from Figure 2: ligands merged into the cleft comprising the TM helix bundle, with the benzyloxy moiety deeply buried within the extracellular half of the TM bundle. This ligand binding mode has already been observed in other docking simulations carried out by some of us using a rhodospin based α_{1d}-AR homology model.[39] According to this docking mode, the charged nitrogen of the ligand anchors the protein scaffold through an electrostatic interaction with Asp176 (3.32), a fundamental receptor recognition point. This interaction is shared by the docking poses selected for all the considered ligands. Furthermore, the presence of the same benzyloxy aromatic moiety favors the stacking of binders towards some essential residues, namely Trp361 (6.48), Phe364 (6.51) and Phe365 (6.52), which are part of TM6. As assessed before, our past efforts[17] aimed at exploring the σ and π effects did not result in any gain of affinity constant. Therefore, it might be postulated that the lonely steric hindrance, provided by this aromatic ring, could probably hamper all the conformational changes of the same helix, which are known to occur for activating the target.[40–43]

The most interesting observations might be done on the receptor complex comprising the ligands disubstituted phenoxy ring, the second extracellular loop (ECL2) and TM7. It has been suggested that the triplet Gly247, Ile248 and Thr249 of the human α_{1d}-AR, highly conserved in the other two subtypes, might be the primary region of binding of antagonists, in agreement with SDM experiments carried out on the equivalent position of the rat α_{1a} and hamster α_{1b}-AR.[44] Comfortably in our docking experiments one o-methoxy group, making significant van der Waals contacts with the side chain of Ile248, can be observed. As a consequence, this incidence might cause a proper orientation of the

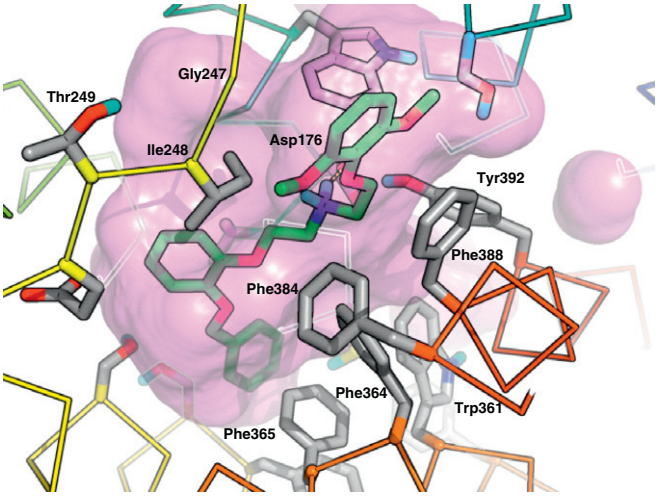

Figure 2. Receptor–ligand complex of α_{1d}-AR and the high affine compound **1**. The surface in magenta represents the void volume of the receptor binding cavity.

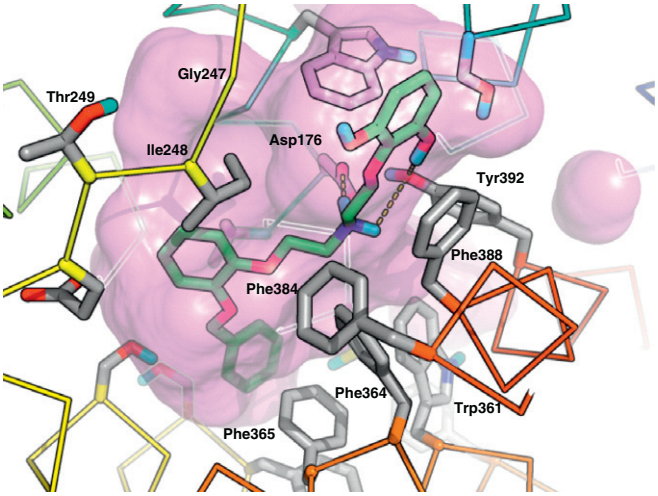

Figure 3. Receptor–ligand complex of α_{1d}-AR and the low affine compound **13**. The surface in magenta represents the void volume of the receptor binding cavity.

disubstituted phenyl ring which is afterward facing Phe384 (7.35) and Phe388 (7.39) arising strong hydrophobic contact (i.e. *face to face* and *edge to face* π–π stacking) with these residues side chains. As further validation of docking poses, SDM experiments also evidenced the aforementioned aminoacids as crucial for ligand binding.[19] All these evidences took place in the docking of **1** and **5**–**14**, in agreement with the importance of shape and polarity as came out from 2D-QSAR. The increase of the steric bulk of the two ortho substituents (**5**) or the replacement of only one methoxy group with different substituents (**6**–**8**) do not dramatically affect the binding mode. In the less affine compounds the mono-substitution (**9**–**10**) or the total absence of o-methoxy groups (**11**–**14**) lock less powerfully the ligand to the binding site. In particular, as shown in Figure 3, the very low α_{1d}-affinity value of the derivative **13** might be due to the presence of the two polar o-hydroxy groups, which might prevent productive interaction with Ile248. Moreover, an additional hydrogen bond with Tyr392 might influence both ligand conformation and ligand–receptor fit and affect the pK_i value.

Also from the docking of compounds **2**–**4** some useful observations came out. In particular, the bioisosteric replacement of the oxygen atom of **1** with a sulfur atom as in **2** preserves the same electron rich hinge pointing towards the antagonists binding region of ECL2 (Fig. S1). Instead the methylene group of **3** or SO moiety of **4**, reducing the electron density on the disubstituted phenyl ring, lowers the strength of the aromatic interaction. Moreover, in the case of **4** the induced reduction of the torsional freedom of the adjacent phenyl-ring also prevents the good fit and π–π stackings with Phe384 (7.35) and Phe388 (7.39) obtained with compounds **1** and **2** (Figs. S2 and S3).

To infer the biological activity profile at three-dimensional level and to produce a sound pharmacophore hypothesis, 3D-QSAR study was performed. To accomplish this goal, docking was used as support tool for chemometric analysis of the measured pK_i. So starting from the docked pose of each complex, a molecular alignment was generated, and affinity constant was related to GRID independent descriptors (GRINDs)[45] measured around the molecules, producing statistical models capable to investigate the molecular determinants most likely affecting the biological data (see Section 4). GRINDs were obtained by a quick and automated procedure involving: (i) computations of the molecular interaction fields (MIFs) induced by selected probe atoms on a 3D grid, (ii) filtering the MIFs in order to extract the most salient chemical information regarding the receptor binding site, and (iii) encoding the spatial relationship within the binding site nodes into new independent 3D variables.

The GRIND descriptors were subsequently used in a Partial Least Squares (PLS) analysis. From the data reported in Table 3 it can be seen that good PLS statistics were obtained, with the percentage of explained variance being almost 95%. Similarly, the q^2 cross-validated correlation coefficients in the Leave-One-Out regression models is well above 0.3 which corresponds to a low probability of chance correlation (i.e. p <5%).

Further insights into the 3D-QSAR results were gained considering signs and magnitudes of the PLS coefficients to determine the chemical descriptors most responsible for antagonist affinity (Fig. 4). This analysis indicates that the MIFs measured at certain grid nodes and exact distances with the N1–TIP, O–TIP, and N1–N1 probes have the greatest impact on antagonist affinity, while variables related to DRY–DRY fields show negative control.

More specifically, variables N1–TIP 7, O–TIP 14 and 40, N1–N1 27 showed the largest coefficients and hence these pharmacophoric moieties are likely to be present in the most affine α_{1d}-AR antagonists and absent in the least affine ones, whereas variable DRY–DRY 49, characterized by a large negative coefficient, should be ascribable to the low affine antagonists (PLS variables in this study were numbered according to the distances between interacting nodes of a given type using a two-digit variable number equal to Å distances by multiplying it by the grid spacing and smoothing window, which were 0.5 and 0.8 Å, respectively).

These results suggested that certain, appropriately spaced, structural elements such as convex molecular surfaces and/or polar functional groups are pivotal for this class of α_{1d}-AR binders, and also that finding an optimal spacing between them might significantly enhance biological affinity. For instance, in the structural model of α_{1d}-AR used for dockings Ile248 $C_{\gamma 1}$ and Asp178 (3.32) $O_{\delta 2}$ are spaced by 5.9 Å; this value seems to resemble field effects measured around affine derivatives (i.e. **1**) with a hydrogen bond acceptor and a shape probe, as scored by variable N1–TIP 7, located in the area surrounding the o-methoxy group and the amino func-

Table 3
Statistical results of PLS analysis for compounds **1**–**14** and WB4101

n	var	Probe	r^2	q^2	s	ONC
15	340	DRY[a] O[b] N1[c] TIP[d]	0.944	0.633	0.168	3

[a] Hydrophobic.
[b] Negatively charged hydrogen bond acceptor.
[c] Neutral hydrogen bond donor.
[d] Shape.

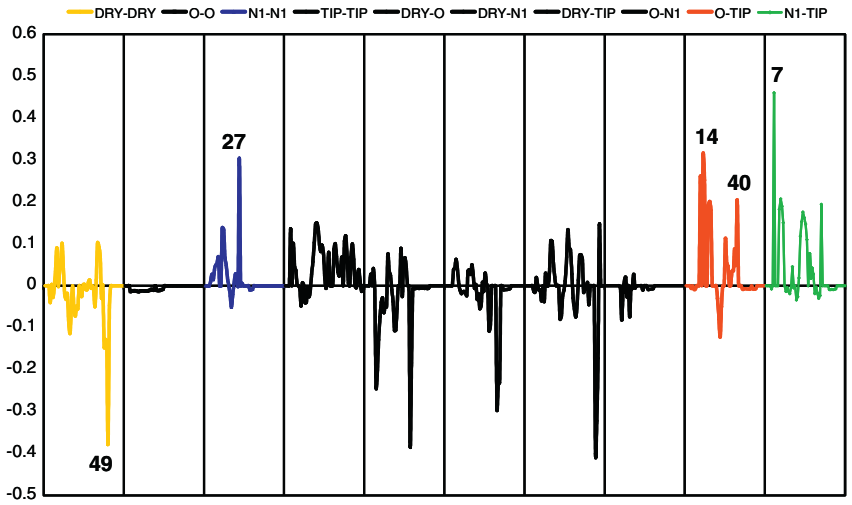

Figure 4. Plot of the PLS coefficients for data set (variables mentioned in the text are highlighted).

tion. Indeed, hydrophobic interactions (π–π stacking) occurring over an intramolecular threshold distance might be detrimental for ligand binding. In fact, the aromatic centroids of Phe365 (6.52) and Phe388 (7.39) are spaced by 11.3 Å that is well below the distance values (19 Å) expressed by variable DRY–DRY 49. Figure 5 shows graphical representations of the above variables displayed for the high and low affine compounds **1** and **13**, respectively.

It was supporting that fields effect emerged from chemometric analysis (i.e. acceptor/donor hydrogen bond) might correspond, to a great extent, to the molecular descriptors (i.e. #NandO) come out as most relevant from the 2D-QSAR study.

In conclusion, comparative modeling and docking experiments, together with QSAR, supported the understanding of α_{1d}-AR binding affinity, elucidating the SAFIR for a series of novel α_{1d}-AR antagonists related to openphendioxan. The pharmacophoric features of the phenoxy terminal most likely capable of enhancing ligands affinity were interpreted with variables encoding the lipopilicity (QPlogBB) and polarity (#NandO) of the substituents. The suggestions of SAFIR regarding a possible lower of pK_i arising from the bioisosteric replacement of the oxygen atom of the bridge spacing the basic centre and the 2,6-dimethoxyphenyl ring with non polar (i.e. methylene) and spatially defined (i.e. SO) groups, or the presence in the phenoxy ring of small substituents at one or both ortho positions were validated by the computational study. Our docking experiments proved that the interaction of the phenoxy moiety of openphendioxan-related compounds is greatly favored by the ortho disubstitution. In particular, two methoxy substituents allow an optimal interaction of the ligand to the binding sites, with one methoxy group forming a specific interaction with the side chain of Ile248 and the other stabilizing a proper orientation of the phenyl ring for strong hydrophobic contacts with Phe384 (7.35) and Phe388 (7.39). Finally, the 3D-QSAR study suggested that properly spaced structural elements, such as convex molecular surface and/or polar functional groups, are pivotal for this class of α_{1d}-AR binders.

4. Experimental section

4.1. Chemistry

Melting points were taken in glass capillary tubes on a Büchi SMP-20 apparatus and are uncorrected. IR and NMR spectra were recorded on Perkin-Elmer 297 and Varian Gemini 200 instruments, respectively. Chemical shifts are reported in parts per million (ppm) relative to tetramethylsilane (TMS), and spin multiplicities are given as s (singlet), d (doublet), dd (double doublet), t (triplet), q (quartet), or m (multiplet). IR spectral data (not shown because of the lack of unusual features) were obtained for all compounds reported and are consistent with the assigned structures. The

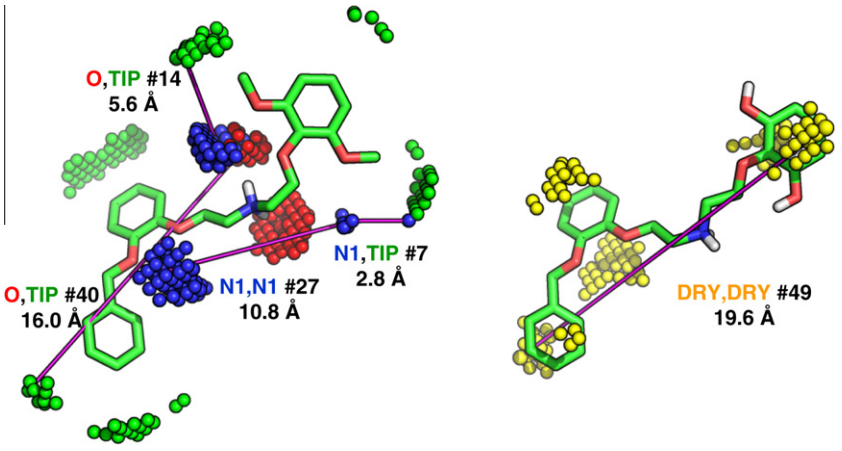

Figure 5. Grid filtered MIFs for the highest affine **1** (left) and low affine **13** (right). The most significant PLS variables 7, 14, 27, 40 and 49 are represented with magenta lines.

microanalyses were performed by the Microanalytical Laboratory of our department. The elemental composition of the compounds agreed to within ±0.4% of the calculated value. Chromatographic separations were performed on silica gel columns (Kieselgel 40, 0.040–0.063 mm, Merck) by flash chromatography. The term 'dried' refers to the use of anhydrous sodium sulfate. Mass spectra were obtained using a Hewlett–Packard 1100 MSD instrument utilizing electron-spray ionization (ESI) and a gas chromatograph/mass spectrometer (GC–MS, EI-70 eV). Compounds were named following IUPAC rules as applied by Beilstein-Institut AutoNom (version 2.1), a software for systematic names in organic chemistry.

4.1.1. 2-(2,6-Dimethoxyphenylthio)acetamide (15)

2,6-Dimethoxybenzenethiol[22] (4.63 g, 27.2 mmol) was added to a solution of Na (0.7 g, 30.4 mmol) in EtOH (120 mL) under mechanical stirring. The mixture was refluxed for 30 min. Then 2-chloroacetamide (2.54 g, 27.2 mmol) and KI (0.5 g) were added and heating was maintained for 5 h. After evaporation of the solvent under vacuum, the residue was treated with 2 N NaOH and extracted with $CHCl_3$. The organic layer was dried over Na_2SO_4 and the solvent was evaporated under vacuum to give a solid: 5.5 g; 96% yield; mp 157–158 °C. ^{1}H NMR ($CDCl_3$): δ 3.52 (s, 2, SCH_2), 3.88 (s, 6, OCH_3), 5.49 and 7.62 (two br t, 2, NH_2, exchangeable with D_2O), 6.55 (d, 2, ArH), 7.28 (t, 1, ArH); MS (ESI) m/z 228.0 ($[M+H]^+$), 250.0 ($[M+Na]^+$).

4.1.2. 2-(2,6-Diethoxyphenoxy)acetamide (16)

A mixture of 2,6-diethoxyphenol[23] (4.07 g, 22.34 mmol), 2-chloroacetamide (2.09 g, 22.34 mmol), and K_2CO_3 (3.09 g, 22.34 mmol) in dry acetone (150 mL) was refluxed for 48 h. After cooling, the solid was filtered and the solvent was evaporated. The residue was dissolved in $CHCl_3$ and washed with 2 N NaOH. Removal of dried solvents gave a solid: 2.53 g; 47% yield; mp 156–157 °C. ^{1}H NMR ($CDCl_3$): δ 1.46 (t, 6, CH_2CH_3), 4.09 (q, 4, CH_2CH_3), 4.57 (s, 2, CH_2CO), 5.72 and 8.01 (two br s, 2, NH_2, exchangeable with D_2O), 6.55 (d, 2, ArH), 6.98 (t, 1, ArH); MS (ESI) m/z 240.1 ($[M+H]^+$), 262.1 ($[M+Na]^+$).

4.1.3. 2-(2-(Benzyloxy)phenoxy)acetamide (17)

This was obtained following the procedure described for **16** starting from 2-(benzyloxy)phenol. The residue was treated with petroleum ether to afford a solid: 65% yield; mp 158–159 °C. ^{1}H NMR ($CDCl_3$): δ 4.52 (s, 2, CH_2CO), 5.08 (s, 2, OCH_2Ar), 5.66 (br s, 2, NH_2, exchangeable with D_2O), 6.83–7.46 (m, 9, ArH); MS (ESI) m/z 258.1 ($[M+H]^+$), 280.1 ($[M+Na]^+$).

4.1.4. 2-(2,6-Dimethoxyphenylthio)ethanamine (18)

A solution of 10 M $BH_3{\cdot}CH_3SCH_3$ (3.0 mL) in dry THF (10 mL) was added dropwise at rt to a stirred solution of **15** (2.0 g, 8.8 mmol) in dry THF (100 mL) under a stream of dry nitrogen with exclusion of moisture. When the addition was completed, the reaction mixture was heated at reflux temperature for 8 h. After the mixture was cooled to 0 °C, excess borane was destroyed by cautious dropwise addition of EtOH (15 mL). The resulting mixture was left to stand overnight at rt, cooled to 0 °C, acidified with concentrated HCl, and then heated to 60 °C for 1 h. Removal of the solvent under reduced pressure gave a residue, which was dissolved in H_2O. The aqueous solution was basified with 2 N NaOH and extracted with $CHCl_3$. Removal of dried solvents gave a residue, which was purified by column chromatography, eluting with $CHCl_3$/EtOH (9.9:0.1) to afford an oil: 1.75 g; 93% yield. ^{1}H NMR ($CDCl_3$): δ 1.62 (br s, 2, NH_2, exchangeable with D_2O), 2.65 and 2.85 (two t, 4, CH_2CH_2), 3.88 (s, 6, OCH_3), 6.57 (d, 2, ArH), 7.27 (t, 1, ArH); MS (ESI) m/z 214.0 ($[M+H]^+$), 236.0 ($[M+Na]^+$).

4.1.5. 2-(2,6-Diethoxyphenoxy)ethanamine (19)

This was obtained following the procedure described for **18** starting from **16**. The free base was transformed into the hydrochloride salt and recrystallized from 2-PrOH: 45% yield; mp 97–98 °C. The hydrochloride salt was dissolved in 2 N NaOH and the solution was extracted with $CHCl_3$. The evaporation of the solvent afforded the pure free base. ^{1}H NMR ($CDCl_3$): δ 1.46 (t, 6, CH_2CH_3), 1.97 (br s, 2, NH_2, exchangeable with D_2O), 2.92 (t, 2, CH_2N), 4.09 (m, 6, CH_2CH_3 and OCH_2), 6.58 (d, 2, ArH), 6.95 (t, 1, ArH); MS (ESI) m/z 226.1 ($[M+H]^+$), 248.1 ($[M+Na]^+$).

4.1.6. 2-(2-(Benzyloxy)phenoxy)ethanamine (20)

This was obtained following the procedure described for **18** starting from **17**. The evaporation of the solvent afforded an oil which was used in the next step without further purification: 81% yield. ^{1}H NMR ($CDCl_3$): δ 1.79 (br s, 2, NH_2, exchangeable with D_2O), 3.07 (t, 2, CH_2N), 4.07 (t, 2, OCH_2), 5.12 (s, 2, OCH_2Ar), 6.82–7.52 (m, 9, ArH); MS (ESI) m/z 244.1 ($[M+H]^+$), 266.1 ($[M+Na]^+$).

4.1.7. 2-(2-(Benzyloxy)phenoxy)-*N*-(2-(2,6-dimethoxyphenylthio)ethyl)acetamide (21)

Et_3N (0.81 mL, 5.81 mmol) and EtOCOCl (0.56 mL, 5.81 mmol) were added to a solution of 2-(2-(benzyloxy)phenoxy)acetic acid[21] (1.5 g, 5.81 mmol) in dry $CHCl_3$ (40 mL) at 0 °C. After 30 min a solution of **18** (1.3 g, 5.81 mmol) in $CHCl_3$ (20 mL) was added and the reaction mixture was left at rt for 3 h. The solution was then washed with 2 N HCl, 2 N NaOH, and the organic phase was dried over Na_2SO_4. Removal of the solvent gave a residue, which was purified by column chromatography. The residue was purified by column chromatography. Eluting with cyclohexane/EtOAc (7:3) afforded an oil: 2.3 g; 88% yield. ^{1}H NMR ($CDCl_3$): δ 2.81 (t, 2, CH_2S), 3.30 (q, 2, NCH_2), 3.81 (s, 6, OCH_3), 4.50 (s, 2, CH_2CO), 5.13 (s, 2, OCH_2Ar), 6.51–7.48 (m, 12, ArH), 7.68 (br t, 1, NH, exchangeable with D_2O); MS (ESI) m/z 454.1 ($[M+H]^+$), 476.1 ($[M+Na]^+$).

4.1.8. 2-(2-(Benzyloxy)phenoxy)-*N*-(2-(2,6-diethoxyphenoxy)ethyl)acetamide (22)

This was obtained following the procedure described for **21** starting from **19**. The residue was purified by column chromatography. Eluting with cyclohexane/EtOAc (8:2) afforded a solid: 68% yield; mp 75–76 °C. ^{1}H NMR ($CDCl_3$): δ 1.33 (t, 6, CH_2CH_3), 3.60 (q, 2, NCH_2), 4.02 (m, 6, CH_2CH_2O and CH_2CH_3), 4.58 (s, 2, CH_2CO), 5.09 (s, 2, OCH_2Ar), 6.46–7.43 (m, 12, ArH), 7.80 (br t, 1, NH, exchangeable with D_2O); MS (ESI) m/z 466.2 ($[M+H]^+$), 488.2 ($[M+Na]^+$).

4.1.9. 2-(2-(Benzyloxy)phenoxy)-*N*-(2-(2-chloro-6-methoxyphenoxy)ethyl)acetamide (23)

This was obtained following the procedure described for **21** starting from 2-(2-chloro-6-methoxyphenoxy)ethanamine.[24] The residue was purified by column chromatography. Eluting with cyclohexane/EtOAc (8:2) afforded an oil: 76% yield. ^{1}H NMR ($CDCl_3$): δ 3.62 (q, 2, NCH_2), 3.72 (s, 3, OCH_3), 4.08 (t, 2, CH_2CH_2O), 4.58 (s, 2, CH_2CO), 5.11 (s, 2, OCH_2Ar), 6.72–7.44 (m, 12, ArH), 7.78 (br t, 1, NH, exchangeable with D_2O); MS (ESI) m/z 442.1 ($[M+H]^+$), 464.1 ($[M+Na]^+$).

4.1.10. 2-(2-(Benzyloxy)phenoxy)-*N*-(2-(2-ethoxyphenoxy)ethyl)acetamide (24)

This was obtained following the procedure described for **21** starting from 2-(2-ethoxyphenoxy)ethanamine. The residue was purified by column chromatography. Eluting with cyclohexane/EtOAc (8:2) afforded a solid: 80% yield; mp 84–85 °C. ^{1}H NMR ($CDCl_3$): δ 1.33 (t, 3, CH_2CH_3), 3.63 (q, 2, NCH_2), 4.02 (m, 4, CH_2CH_2O and OCH_2CH_3), 4.58 (s, 2, CH_2CO), 5.10 (s, 2, OCH_2Ar), 6.82–7.44 (m,

13, ArH), 7.52 (br t, 1, NH, exchangeable with D_2O); MS (ESI) *m*/*z* 422.1 ($[M+H]^+$), 444.1 ($[M+Na]^+$).

4.1.11. 2-(2-(Benzyloxy)phenoxy)-*N*-(2-(2-methoxyphenoxy) ethyl)acetamide (25)

This was obtained following the procedure described for **21** starting from 2-(2-methoxyphenoxy)ethanamine. The residue was purified by column chromatography. Eluting with cyclohexane/EtOAc (7:3) afforded a solid: 76% yield; 75–76 °C. ^1H NMR ($CDCl_3$): δ 3.62 (q, 2, NCH_2), 3.71 (s, 3, OCH_3), 4.0 (t, 2, CH_2CH_2O), 4.52 (s, 2, CH_2CO), 5.07 (s, 2, OCH_2Ar), 6.79–7.42 (m, 14, ArH and NH, exchangeable with D_2O); MS (ESI) *m*/*z* 408.1 ($[M+H]^+$), 430.1 ($[M+Na]^+$).

4.1.12. 2-(2-(Benzyloxy)phenoxy)-*N*-(2-(2,6-dichlorophenoxy) ethyl)acetamide (26)

This was obtained following the procedure described for **21** starting from 2-(2,6-dichlorophenoxy)ethanamine.[24] The residue was purified by column chromatography. Eluting with cyclohexane/EtOAc (8.5:1.5) afforded a solid which was crystallized from cyclohexane: 60% yield; mp 112–113 °C. ^1H NMR ($CDCl_3$): δ 3.68 (q, 2, NCH_2), 4.05 (t, 2, CH_2CH_2O), 4.60 (s, 2, CH_2CO), 5.12 (s, 2, OCH_2Ar), 6.92–7.46 (m, 12, ArH), 7.69 (br t, 1, NH, exchangeable with D_2O); MS (ESI) *m*/*z* 446.0 ($[M+H]^+$), 468.0 ($[M+Na]^+$).

4.1.13. 2-(2-(Benzyloxy)phenoxy)-*N*-(2-(2,6-dimethylphenoxy) ethyl)acetamide (27)

This was obtained following the procedure described for **21** starting from 2-(2,6-dimethylphenoxy)ethanamine. Removal of the solvent gave a residue, which was purified by column chromatography. Eluting with cyclohexane/EtOAc (8:2) afforded a solid: 47% yield; mp 95–96 °C. ^1H NMR ($CDCl_3$): δ 2.18 (s, 6, CH_3), 3.65 (q, 2, NCH_2), 3.76 (t, 2, CH_2CH_2O), 4.60 (s, 2, CH_2CO), 5.09 (s, 2, OCH_2Ar), 6.84–7.43 (m, 12, ArH), 7.63 (br t, 1, NH, exchangeable with D_2O); MS (ESI) *m*/*z* 406.1 ($[M+H]^+$), 428.1 ($[M+Na]^+$).

4.1.14. 2-(2-(Benzyloxy)phenoxy)-*N*-(2-phenoxyethyl)acetamide (28)

This was obtained following the procedure described for **21** starting from 2-phenoxyethanamine. The residue was purified by column chromatography. Eluting with cyclohexane/EtOAc (7:3) afforded a solid: 71% yield; 103–104 °C. ^1H NMR ($CDCl_3$): δ 3.60 (q, 2, NCH_2), 3.92 (t, 2, CH_2CH_2O), 4.52 (s, 2, CH_2CO), 5.08 (s, 2, OCH_2Ar), 6.72–7.52 (m, 15, ArH and NH, exchangeable with D_2O); MS (ESI) *m*/*z* 378.1 ($[M+H]^+$), 400.1 ($[M+Na]^+$).

4.1.15. *N*-(2-(2-(Benzyloxy)phenoxy)ethyl)-3-(2,6-dimethoxy phenyl)propanamide (29)

This was obtained following the procedure described for **21** starting from **20** and 3-(2,6-dimethoxyphenyl)propanoic acid.[25] The residue was purified by column chromatography. Eluting with cyclohexane/EtOAc (7:3) afforded a solid: 45% yield; mp 114–115 °C. ^1H NMR ($CDCl_3$): δ 2.38 (t, 2, $COCH_2$), 2.91 (t, 2, $COCH_2CH_2$), 3.63 (q, 2, NCH_2), 3.75 (s, 6, OCH_3), 4.06 (t, 2, OCH_2CH_2), 5.08 (s, 2, OCH_2Ar), 6.38 (br t, 1, NH, exchangeable with D_2O), 6.43–7.44 (m, 12, ArH); MS (ESI) *m*/*z* 436.2 ($[M+H]^+$), 458.2 ($[M+Na]^+$).

4.1.16. *N*-(2-(2-(Benzyloxy)phenoxy)ethyl)-2-(2-methoxy-6-nitrophenoxy)acetamide (30)

This was obtained following the procedure described for **21** starting from **20** and 2-(2-methoxy-6-nitrophenoxy)acetic acid.[26] The residue was purified by column chromatography. Eluting with cyclohexane/EtOAc (5:5) afforded an oil: 65% yield. ^1H NMR ($CDCl_3$): δ 3.78 (s, 3, OCH_3), 3.80 (q, 2, NCH_2), 4.20 (t, 2, OCH_2CH_2), 4.61 (s, 2, $COCH_2$), 5.08 (s, 2, OCH_2Ar), 6.90–7.43 (m, 12, ArH), 7.56 (br t, 1, NH, exchangeable with D_2O); MS (ESI) *m*/*z* 453.1 ($[M+H]^+$), 475.1 ($[M+Na]^+$).

4.1.17. *N*-(2-(2-(Benzyloxy)phenoxy)ethyl)-2-(2-methoxy-6-methylphenoxy)acetamide (31)

This was obtained following the procedure described for **21** starting from **20** and 2-(2-methoxy-6-methylphenoxy)acetic acid.[27] The residue was purified by column chromatography. Eluting with cyclohexane/EtOAc (7:3) afforded an oil: 76% yield. ^1H NMR ($CDCl_3$): δ 2.22 (s, 3, CH_3Ar), 3.72 (s, 3, OCH_3), 3.82 (q, 2, NCH_2), 4.20 (t, 2, OCH_2CH_2), 4.42 (s, 2, $COCH_2$), 5.09 (s, 2, OCH_2Ar), 6.64–7.40 (m, 12, ArH), 7.87 (br t, 1, NH, exchangeable with D_2O); MS (ESI) *m*/*z* 422.1 ($[M+H]^+$), 444.1 ($[M+Na]^+$).

4.1.18. *N*-(2-(2-(Benzyloxy)phenoxy)ethyl)-2-(2,6-bis(methoxy methoxy)phenoxy)acetamide (32)

This was obtained following the procedure described for **21** starting from **20** and **35**. The residue was purified by column chromatography. Eluting with cyclohexane/EtOAc (7:3) afforded an oil: 58% yield. ^1H NMR ($CDCl_3$): δ 3.41 (s, 6, OCH_3), 3.80 (q, 2, CH_2N), 4.18 (t, 2, OCH_2CH_2), 4.58 (s, 2, $COCH_2$), 5.10 (s, 2, OCH_2Ar), 5.13 (s, 4, OCH_2O), 6.78–7.43 (m, 12, ArH), 8.31 (br t, 1 NH, exchangeable with D_2O); MS (ESI) *m*/*z* 498.2 ($[M+H]^+$), 520.2 ($[M+Na]^+$).

4.1.19. 2-(2-(Benzyloxy)phenoxy)-*N*-(2-(2,6-dimethoxyphenylthio)ethyl)ethanamine (2)

This was obtained following the procedure described for **18** starting from **21**. The residue was purified by column chromatography. Eluting with $CHCl_3$/EtOH (9.9:0.1) afforded the free base as an oil: 52% yield. ^1H NMR ($CDCl_3$): δ 2.02 (br s, 1, NH, exchangeable with D_2O), 2.70 (t, 2, CH_2S), 2.95 and 2.99 (two t, 4, CH_2NCH_2), 3.85 (s, 6, OCH_3), 4.12 (t, 2, OCH_2CH_2), 5.12 (s, 2, OCH_2Ar), 6.52–7.49 (m, 12, ArH); MS (ESI) *m*/*z* 440.1 ($[M+H]^+$), 462.1 ($[M+Na]^+$. The free base was transformed into the oxalate salt and recrystallized from EtOH; mp 161–162 °C. Anal. Calcd for $C_{25}H_{29}NO_4S\cdot C_2H_2O_4$: C, 61.23; H, 5.90; N, 2.64; S, 6.05. Found: C, 61.03; H, 6.19; N, 2.88; S, 5.86.

4.1.20. 2-(2-(Benzyloxy)phenoxy)-*N*-(2-(2,6-dimethoxyphenyl sulfinyl)ethyl)ethanamine (4)

A solution of **2** (0.36 g, 0.82 mmol), glacial AcOH (0.3 mL) and 30% H_2O_2 (0.4 mL) was left at rt for 9 h. The solution was basified with 2 N NaOH, extracted with $CHCl_3$ and the organic solvents were dried over Na_2SO_4. After evaporation of the solvent, the residue was purified by column chromatography. Eluting with $CHCl_3$/EtOH (9.9:0.1) afforded the free base as an oil: 35% yield. ^1H NMR ($CDCl_3$): δ 1.79 (br s, 1, NH, exchangeable with D_2O), 3.0–3.26 (m, 6, $CH_2NCH_2CH_2S$), 3.86 (s, 6, OCH_3), 4.12 (t, 2, OCH_2CH_2), 5.09 (s, 2, OCH_2Ar), 6.52–7.49 (m, 12, ArH); MS (ESI) *m*/*z* 456.1 ($[M+H]^+$), 478.1 ($[M+Na]^+$). The free base was transformed into the oxalate salt and recrystallized from 2-PrOH; mp 146–147 °C. Anal. Calcd for $C_{25}H_{29}NO_5S\cdot C_2H_2O_4\cdot 0.5H_2O$: C, 58.47; H, 5.82; N, 2.53; S, 5.78. Found: C, 58.60; H, 5.93; N, 2.52; S, 6.12.

4.1.21. *N*-(2-(2-(Benzyloxy)phenoxy)ethyl)-3-(2,6-dimethoxy phenyl)propan-1-amine (3)

This was obtained following the procedure described for **18** starting from **29**. The residue was purified by column chromatography. Eluting with $CHCl_3$/EtOH (9.9:0.1) afforded the free base as an oil: 63% yield. ^1H NMR ($CDCl_3$): δ 1.75 (quintet, 2, $CH_2CH_2CH_2$), 1.91 (br s, 1, NH, exchangeable with D_2O), 2.67 (m, 4, CH_2NCH_2), 3.02 (t, 2, CH_2Ar), 3.79 (s, 6, OCH_3), 4.15 (t, 2, OCH_2CH_2), 5.12 (s, 2, OCH_2Ar), 6.48–7.49 (m, 12, ArH); MS (ESI) *m*/*z* 422.2 ($[M+H]^+$), 444.2 ($[M+Na]^+$). The free base was transformed into the oxalate salt and recrystallized from 2-PrOH; mp

159–160 °C. Anal. Calcd for $C_{26}H_{31}NO_4 \cdot C_2H_2O_4$: C, 65.74; H, 6.50; N, 2.74. Found: C, 65.92; H, 6.82; N, 2.88.

4.1.22. 2-(2-(Benzyloxy)phenoxy)-*N*-(2-(2,6-diethoxyphenoxy) ethyl)ethanamine (5)

This was obtained following the procedure described for **18** starting from **22**. The residue was purified by column chromatography. Eluting with $CHCl_3$/EtOH (9.9:0.1) afforded the free base as an oil: 83% yield. ^1H NMR ($CDCl_3$): δ 1.41 (t, 6, CH_2CH_3), 2.38 (br s, 1, NH, exchangeable with D_2O), 3.01 and 3.13 (two t, 4, CH_2NCH_2), 4.03 (q, 4, CH_2CH_3), 4.18 (m, 4, OCH_2 and CH_2O), 5.12 (s, 2, OCH_2Ar), 6.50–7.44 (m, 12, ArH); MS (ESI) *m*/*z* 452.2 ($[M+H]^+$), 474.2 ($[M+Na]^+$). The free base was transformed into the oxalate salt and recrystallized from 2-PrOH; mp 109–110 °C. Anal. Calcd for $C_{27}H_{33}NO_5 \cdot C_2H_2O_4$: C, 64.31; H, 6.51; N, 2.59. Found: C, 63.97; H, 6.82; N, 2.67.

4.1.23. 2-(2-(Benzyloxy)phenoxy)-*N*-(2-(2-methoxy-6-nitrophen oxy)ethyl)ethanamine (6)

This was obtained following the procedure described for **18** starting from **30**. The residue was purified by column chromatography. Eluting with $CHCl_3$/EtOH (9.7:0.3) afforded the free base as an oil: 60% yield. ^1H NMR ($CDCl_3$): δ 2.81 (br s, 1, NH, exchangeable with D_2O), 3.25 and 3.32 (two t, 4, CH_2NCH_2), 3.84 (s, 3, OCH_3), 4.35 (m, 4, OCH_2 and CH_2O), 5.08 (s, 2, OCH_2Ar), 6.88–7.47 (m, 12, ArH); MS (ESI) *m*/*z* 439.1 ($[M+H]^+$), 461.1 ($[M+Na]^+$). The free base was transformed into the oxalate salt and recrystallized from EtOH; mp 161–162 °C. Anal. Calcd for $C_{24}H_{26}N_2O_6 \cdot C_2H_2O_4$: C, 59.09; H, 5.34; N, 5.30. Found: C, 59.09; H, 5.53; N, 5.34.

4.1.24. 2-(2-(Benzyloxy)phenoxy)-*N*-(2-(2-chloro-6-methoxy phenoxy)ethyl)ethanamine (7)

This was obtained following the procedure described for **18** starting from **23**. The residue was purified by column chromatography. Eluting with $CHCl_3$/EtOH (9.9:0.1) afforded the free base as an oil: 80% yield. ^1H NMR ($CDCl_3$): δ 2.14 (br s, 1, NH, exchangeable with D_2O), 3.07 and 3.13 (two t, 4, CH_2NCH_2), 3.78 (s, 3, OCH_3), 4.18 (m, 4, OCH_2 and CH_2O), 5.12 (s, 2, OCH_2Ar), 6.72–7.47 (m, 12, ArH); MS (ESI) *m*/*z* 428.1 ($[M+H]^+$), 450.1 ($[M+Na]^+$). The free base was transformed into the oxalate salt and recrystallized from EtOH; mp 151–152 °C. Anal. Calcd for $C_{24}H_{26}ClNO_4 \cdot C_2H_2O_4$: C, 60.29; H, 5.45; N, 2.70. Found: C, 59.97; H, 5.71; N, 2.75.

4.1.25. 2-(2-(Benzyloxy)phenoxy)-*N*-(2-(2-methoxy-6-methyl phenoxy)ethyl)ethanamine (8)

This was obtained following the procedure described for **18** starting from **31**. The residue was purified by column chromatography. Eluting with $CHCl_3$/EtOH (9.9:0.1) afforded the free base as an oil: 74% yield. ^1H NMR ($CDCl_3$): δ 2.15 (s, 3, CH_3), 2.72 (br s, 1, NH, exchangeable with D_2O), 3.05 and 3.13 (two t, 4, CH_2NCH_2), 3.78 (s, 3, OCH_3), 4.02 and 4.20 (two t, 4, OCH_2 and CH_2O), 5.08 (s, 2, OCH_2Ar), 6.67–7.42 (m, 12, ArH); MS (ESI) *m*/*z* 408.2 ($[M+H]^+$), 430.2 ($[M+Na]^+$). The free base was transformed into the oxalate salt and recrystallized from EtOH; mp 164–165 °C. Anal. Calcd for $C_{25}H_{29}NO_4 \cdot C_2H_2O_4$: C, 65.18; H, 6.28; N, 2.82. Found: C, 64.94; H, 6.65; N, 2.88.

4.1.26. 2-(2-(Benzyloxy)phenoxy)-*N*-(2-(2-ethoxyphenoxy) ethyl)ethanamine (9)

This was obtained following the procedure described for **18** starting from **24**. The residue was purified by column chromatography. Eluting with $CHCl_3$/EtOH (9.9:0.1) afforded the free base as an oil: 67% yield. ^1H NMR ($CDCl_3$): δ 1.40 (t, 3, CH_2CH_3), 1.92 (br s, 1, NH, exchangeable with D_2O), 3.11 (m, 4, CH_2NCH_2), 4.03 (q, 2, CH_2CH_3), 4.13 (m, 4, OCH_2 and CH_2O), 5.11 (s, 2, OCH_2Ar), 6.81–7.48 (m, 13, ArH); MS (ESI) *m*/*z* 408.2 ($[M+H]^+$), 430.2 ($[M+Na]^+$). The free base was transformed into the oxalate salt and recrystallized from EtOH; mp 164–165 °C. Anal. Calcd for $C_{25}H_{29}NO_4 \cdot C_2H_2O_4$: C, 65.18; H, 6.28; N, 2.82. Found: C, 64.95; H, 6.57; N, 2.89.

4.1.27. 2-(2-(Benzyloxy)phenoxy)-*N*-(2-(2-methoxyphenoxy) ethyl)ethanamine (10)

This was obtained following the procedure described for **18** starting from **25**. The residue was purified by column chromatography. Eluting with $CHCl_3$/EtOH (9.9:0.1) afforded the free base as an oil: 72% yield. ^1H NMR ($CDCl_3$): δ 2.42 (br s, 1, NH, exchangeable with D_2O), 3.10 (m, 4, CH_2NCH_2), 3.77 (s, 3, OCH_3), 4.08 and 4.18 (two t, 4, OCH_2 and CH_2O), 5.09 (s, 2, OCH_2Ar), 6.79–7.43 (m, 13, ArH); MS (ESI) *m*/*z* 394.1 ($[M+H]^+$), 416.1 ($[M+Na]^+$). The free base was transformed into the oxalate salt and recrystallized from EtOH; mp 199–200 °C. Anal. Calcd for $C_{24}H_{27}NO_4 \cdot C_2H_2O_4 \cdot 0.25H_2O$: C, 63.99; H, 6.09; N, 2.87. Found: C, 63.96; H, 6.38; N, 2.70.

4.1.28. 2-(2-(Benzyloxy)phenoxy)-*N*-(2-(2,6-dichlorophenoxy) ethyl)ethanamine (11)

This was obtained following the procedure described for **18** starting from **26**. The residue was purified by column chromatography. Eluting with $CHCl_3$/EtOH (9.9:0.1) afforded the free base as a solid: 56% yield; mp 66–67 °C. ^1H NMR ($CDCl_3$): δ 2.60 (br s, 1, NH, exchangeable with D_2O), 3.20 and 3.27 (two t, 4, CH_2NCH_2), 4.21 and 4.30 (two t, 4, OCH_2 and CH_2O), 5.12 (s, 2, OCH_2Ar), 6.88–7.46 (m, 12, ArH); MS (ESI) *m*/*z* 432.1 ($[M+H]^+$), 454.1 ($[M+Na]^+$). The free base was transformed into the oxalate salt and recrystallized from EtOH; mp 157–158 °C. Anal. Calcd for $C_{23}H_{23}Cl_2NO_3 \cdot C_2H_2O_4$: C, 57.48; H, 4.82; N, 2.68. Found: C, 57.61; H, 5.15; N, 2.73.

4.1.29. 2-(2-(Benzyloxy)phenoxy)-*N*-(2-(2,6-dimethylphenoxy) ethyl)ethanamine (12)

This was obtained following the procedure described for **18** starting from **27**. The residue was purified by column chromatography. Removal of dried solvents gave a residue, which was purified by column chromatography, eluting with $CHCl_3$/EtOH (9.9:0.1) to afford an oil: 0.5 g; 79% yield. ^1H NMR ($CDCl_3$): δ 2.26 (s, 6, CH_3), 2.52 (br s, 1, NH, exchangeable with D_2O), 3.12 and 3.20 (two t, 4, CH_2NCH_2), 3.88 and 4.24 (two t, 4, OCH_2 and CH_2O), 5.11 (s, 2, OCH_2Ar), 6.88–7.45 (m, 12, ArH); MS (ESI) *m*/*z* 392.2 ($[M+H]^+$), 414.1 ($[M+Na]^+$). The free base was transformed into the oxalate salt and recrystallized from MeOH; mp 180–181 °C. Anal. Calcd for $C_{25}H_{29}NO_3 \cdot C_2H_2O_4$: C, 67.34; H, 6.49; N, 2.91. Found: C, 67.10; H, 6.68; N, 2.96.

4.1.30. 2-(2-(2-(2-(Benzyloxy)phenoxy)ethylamino)ethoxy) benzene-1,3-diol (13)

This was obtained following the procedure described for **18** starting from **32**. The residue was purified by column chromatography. Eluting with $CHCl_3$/EtOH (8.5:1.5) afforded the free base as a solid: 60% yield; mp 118–119 °C. ^1H NMR ($CDCl_3$): δ 2.88 and 3.08 (two t, 4, CH_2NCH_2), 3.91 and 4.20 (two t, 4, OCH_2 and CH_2O), 5.07 (s, 2, OCH_2Ar), 5.20 (br s, 1 NH, exchangeable with D_2O), 6.42–7.48 (m, 14, OH and ArH); MS (ESI) *m*/*z* 396.1 ($[M+H]^+$), 418.1 ($[M+Na]^+$). The free base was transformed into the oxalate salt and recrystallized from 2-PrOH; mp 113–114 °C. Anal. Calcd for $C_{23}H_{25}NO_5 \cdot C_2H_2O_4$: C, 61.85; H, 5.61; N, 2.89. Found: C, 61.58; H, 5.33; N, 2.93.

4.1.31. 2-(2-(Benzyloxy)phenoxy)-*N*-(2-phenoxyethyl)ethan amine (14)

This was obtained following the procedure described for **18** starting from **28**. The residue was purified by column chromatography.

Eluting with $CHCl_3$/EtOH (9.8:0.2) afforded the free base as a solid: 80% yield; mp 40–41 °C. ^{1}H NMR ($CDCl_3$): δ 1.31 (br s, 1, NH, exchangeable with D_2O), 3.08 (m, 4, CH_2NCH_2), 4.02 and 4.15 (two t, 4, OCH_2 and CH_2O), 5.09 (s, 2, OCH_2Ar), 6.89–7.45 (m, 14, ArH); MS (ESI) *m*/*z* 364.1 ([M+H]$^+$), 386.1 ([M+Na]$^+$). The free base was transformed into the oxalate salt and recrystallized from EtOH; mp 195–196 °C. Anal. Calcd for $C_{23}H_{25}NO_3{\cdot}C_2H_2O_4{\cdot}0.5H_2O$: C, 64.92; H, 6.10; N, 3.03. Found: C, 65.17; H, 6.47; N, 2.93.

4.1.32. 2,6-Bis(methoxymethoxy)phenol (33)

1.6 M *n*-Butillitium (14 mL) was added to an ice-cooled solution of 1,3-bis(methoxymethoxy)benzene[28] (3.16 g, 15.21 mmol) in dry THF (50 mL) under nitrogen. After stirring for 1 h at rt, the solution was cooled to 0 °C and trimethyl borate (1.52 g, 25.51 mmol) was added. After 30 min under stirring the solution was concentrated under vacuum and the crude residue was dissolved in 20% aqueous acetone (54 mL) containing $NaHCO_3$ (15.14 g). Oxone (3.8 g) was added and stirring continued. After 5 min $NaHSO_3$ (2.09 g) was added. The reaction mixture was extracted with EtOAc and dried over Na_2SO_4. Evaporation of the solvent gave an oil, which was purified by column chromatography. Eluting with cyclohexane/EtOAc (9:1) afforded **33** as an oil: 1.11 g; 33% yield. ^{1}H NMR ($CDCl_3$): δ 3.52 (s, 6, OCH_3), 5.20 (s, 4, OCH_2), 6.63–6.84 (m, 4, OH and ArH); MS (ESI) *m*/*z* 213.0 ([M−H]$^-$).

4.1.33. Methyl 2-(2,6-bis(methoxymethoxy)phenoxy)acetate (34)

A mixture of **33** (1.11 g, 5.18 mmol) methyl 2-chloroacetate (0.53 mL, 6.06 mmol), K_2CO_3 (0.84 g, 6.06 mmol) and KI (0.106 g) in dry acetone (40 mL) was refluxed for 13 h. After cooling the solid was filtered and the filtrate was evaporated. The residue was dissolved in EtOAc, was washed with 2 N NaOH and the organic layer was dried over Na_2SO_4. After evaporation of the solvent the residue was purified by column chromatography. Eluting with cyclohexane/EtOAc (9:1) afforded an oil: 1.1 g; yield = 74%. ^{1}H NMR ($CDCl_3$): δ 3.52 (s, 6, OCH_3), 3.80 (s, 3, $COOCH_3$), 4.66 (s, 2, CH_2CO), 5.20 (s, 4, OCH_2O), 6.81–7.02 (m, 3, ArH); MS (EI) *m*/*z* 286 [M$^+$], 254, 227, 213, 121, 62, 45 (100), 39.

4.1.34. 2-(2,6-Bis(methoxymethoxy)phenoxy)acetic acid (35)

A mixture of **34** (1.0 g; 3.49 mmol) and 2 N NaOH (40 mL) was stirred at 70 °C for 3 h. After cooling to 0 °C, 2 N HCl was added till pH 7 followed by NH_4Cl saturated solution till pH 4–5. Extraction with $CHCl_3$ followed by washing, drying, and evaporation of the extracts gave an oil: 0.85 g; 81% yield. ^{1}H NMR ($CDCl_3$): δ 3.52 (s, 6, OCH_3), 4.66 (s, 2, CH_2CO), 5.25 (s, 4, OCH_2O), 6.87 (d, 2, ArH), 7.02 (t, 1, ArH), 7.65 (br s, 1, COOH, exchangeable with D_2O); MS (ESI) *m*/*z* 271.0 ([M−H]$^-$).

4.2. Pharmacology

4.2.1. Functional antagonism in isolated tissues

Male Wistar rats (275–300 g) were killed by cervical dislocation, and the organs required were isolated, freed from adhering connective tissue, and set up rapidly under a suitable resting tension in 20 mL organ baths containing physiological salt solution kept at 37 °C and aerated with 5% CO_2:95% O_2 at pH 7.4. Concentration-response curves were constructed by cumulative addition of agonist. The concentration of agonist in the organ bath was increased approximately threefold at each step, with each addition being made only after the response to the previous addition had attained a maximal level and remained steady. Contractions were recorded by means of a force displacement transducer connected to the MacLab system PowerLab/800. In addition, parallel experiments in which tissues did not receive any antagonist were run in order to check any variation in sensitivity.

4.2.1.1. Rat vas deferens prostatic portion. This tissue was used to assess α_{1A}-adrenergic antagonism.[32] Prostatic portions of 2 cm length were mounted under 0.5 g of tension in Tyrode solution of the following composition (mM): NaCl, 130.0; KCl, 2.0; $CaCl_2$, 1.8; $MgCl_2$, 0.89; $NaHCO_3$, 25.0; NaH_2PO_4, 0.42; glucose, 5.6. Cocaine hydrochloride (0.1 μM) was added to the Tyrode to prevent the neuronal uptake of (−)-noradrenaline. The preparations were equilibrated for 60 min with washing every 15 min. After the equilibration period, tissues were primed two times by addition of 10 μM (−)-noradrenaline. After another washing and equilibration period of 60 min, a (−)-noradrenaline concentration-response curve was constructed (basal response). The antagonist was allowed to equilibrate with the tissue for 30 min, followed by 30 min of washing. Then, a new concentration-response curve to the agonist was obtained. (−)-Noradrenaline solutions contained 0.05% $Na_2S_2O_5$ to prevent oxidation.

4.2.1.2. Rat spleen. This tissue was used to assess α_{1B}-adrenergic antagonism.[34] The spleen was removed and bisected longitudinally into two strips, which were suspended in tissue baths containing Krebs solution of the following composition (mM): NaCl, 120.0; KCl, 4.7; $CaCl_2$, 2.5; $MgSO_4$, 1.5; $NaHCO_3$, 20.0; KH_2PO_4, 1.2; glucose, 11.0; K_2ethylenediaminetetraacetic acid (EDTA), 0.01. (±)-Propranolol hydrochloride (4.0 μM) was added to block β-ARs. The spleen strips were placed under 1 g of resting tension and equilibrated for 2 h. The cumulative concentration-response curves to (−)-phenylephrine were measured isometrically and obtained at 30 min intervals; the first one was discarded, and the second one was taken as the control. The antagonist was allowed to equilibrate with the tissue for 30 min, followed by 30 min of washing. Then, a new concentration-response curve to the agonist was constructed.

4.2.1.3. Rat aorta. This tissue was used to assess α_{1D}-adrenergic antagonism.[33] Thoracic aorta was cleaned from extraneous connective tissue and placed in Krebs solution of the following composition (mM): NaCl, 118.4; KCl, 4.7; $CaCl_2$, 1.9; $MgSO_4$, 1.2; $NaHCO_3$, 25.0; NaH_2PO_4, 1.2; glucose, 11.7. Cocaine hydrochloride (0.1 μM) and (±)-propranolol hydrochloride (4.0 μM) were added to prevent the neuronal uptake of (−)-noradrenaline and to block β-ARs, respectively. Two helicoidal strips (15 × 3 mm) were cut from each aorta beginning from the end most proximal to the heart. The endothelium was removed by rubbing with filter paper; the absence of acetylcholine (100 μM)-induced relaxation to preparations contracted with (−)-noradrenaline (1 μM) was taken as an indicator that the vessel was denuded successfully. Vascular strips were then tied with surgical thread and suspended in a jacketed tissue bath containing Tyrode solution. Strips were secured at one end to Plexiglas hooks and connected to a transducer for monitoring changes in isometric contraction. After at least 2 h equilibration period under an optimal tension of 2 g, cumulative (−)-noradrenaline concentration-response curves were recorded at 1 h intervals; the first two were discarded, and the third one was taken as the control. The antagonist was allowed to equilibrate with the tissue for 30 min before the generation of the fourth cumulative concentration-response curve to (−)-noradrenaline. (−)-Noradrenaline solutions contained 0.05% K_2EDTA and 0.9% NaCl to prevent oxidation.

4.2.2. Binding studies

4.2.2.1. Radioligand binding assays. Binding to cloned human α_1-AR subtypes was performed in membranes from CHO cells transfected by electroporation with DNA expressing the gene encoding each α_1-AR subtype. Cloning and stable expression of the human α_1-AR gene was performed as previously described.[29] CHO cell membranes (30 μg proteins) were incubated in 50 mM

Tris–HCl, pH 7.4, with 0.1–0.4 nM [^3H]prazosin, in a final volume of 1.02 mL for 30 min at 25 °C, in absence or presence of competing drugs (1 pM–10 μM). Nonspecific binding was determined in the presence of 10 μM phentolamine. The incubation was stopped by addition of ice-cold Tris–HCl buffer and rapid filtration through 0.2% polyethyleneimine-pretreated Whatman GF/B or Schleicher & Schuell GF52 filters. Genomic clone G-21 coding for the human 5-HT_{1A} receptor was stably transfected in a human cell line (HeLa).[30] HeLa cells were grown as monolayers in Dulbecco's modified Eagle's medium (DMEM), supplemented with 10% fetal calf serum and gentamicin (100 μg/mL), and 5% CO_2 at 37 °C. Cells were detached from the growth flask at 95% confluence by a cell scraper and were lysed in ice-cold Tris 5 mM and EDTA 5 mM buffer (pH 7.4). Homogenates were centrifuged at 40,000*g* for 20 min, and pellets were resuspended in a small volume of ice-cold Tris 5 mM and EDTA 5 mM buffer (pH 7.4) and immediately frozen and stored at −70 °C until use. On the experimental day, cell membranes were resuspended in binding buffer: 50 mM Tris–HCl (pH 7.4), 2.5 mM $MgCl_2$, and 10 μM pargiline.[31] Membranes were incubated in a final volume of 1 mL for 30 min at 30 °C with 0.7–1.4 nM [^3H]8-OH-DPAT, in the absence or presence of competing drugs. Nonspecific binding was determined in the presence of 10 μM 5-HT. The incubation was stopped by the addition of ice-cold Tris–HCl buffer and rapid filtration through 0.2% polyethyleneimine-pretreated Whatman GF/B or Schleicher & Schuell GF52 filters.

4.2.3. Data analysis

In functional studies, responses were expressed as percentage of the maximal contraction observed in the agonist concentration-response curve taken as a control. The agonist concentration-response curves were analyzed by pharmacological computer programs. pK_b values were calculated from only one concentration. Compounds **2**–**14** were tested at only one concentration, in the range of 0.01–10 μM, when determining α_1-AR blocking activity. pK_b values were calculated according to van Rossum.[46]

Binding data were analyzed using the nonlinear curve-fitting program Allfit.[47] Scatchard plots were linear in all preparations. All pseudo-Hill coefficients (nH) were not significantly different from unity (p >0.05). Equilibrium inhibition constants (K_i) were derived from the Cheng–Prusoff[48] Equation: $K_i = IC_{50}/(1 + L/K_d)$, where L and K_d are the concentration and the equilibrium dissociation constant of the radioligand. pK_i values are the mean ± SE of 2–3 separate experiments performed in triplicate.

4.3. Modeling study

In the 2D-QSAR statistical analysis was performed relating pK_i with the fifty QikProp molecular descriptors by multiple linear regression, automatically selecting the optimal subset of variables and removing any outlier. A ratio of one variable per eight compounds was applied. Molecular structures of the protonated compounds **1**–**14** were built using the Flo+ suite of software[49] with standard bond distances and valence angles, while for WB 4101 the X-ray structure of the (*S*)-enantiomer was used in calculations (CSD code: BAXBEH). The α_{1d}-AR model was built by comparative modeling (by means of MODELLER 7v7)[50] by using the crystal structure of β_2-AR as a template. All the receptor domains but N-term, third intracellular loop and C-term were modeled (i.e. the 92–419 sequence). A modified β_2-AR template was used lacking the amino acid segments 176–190 and 263–265. External α-helical restraints were imposed to the 415–419 sequence. Moreover, a disulphide bridge patch was employed between C169 (3.25) and C244. The best α_{1d}-AR model was subjected to rotations of the amino acid side chains when in non allowed conformations and then subjected to energy minimization, by using the GBSW implicit membrane/water model.[51] With respect to the physical parameters representing the membrane, the surface tension coefficient (representing the non-polar solvation energy) was set to 0.03 kcal/(mol.A2). The membrane thickness centered at $Z = 0$ was set to 30.0 Å with a membrane smoothing length of 5.0 Å (wm = 2.5 Å). Minimizations were carried out by using 1500 steps of steepest descent followed by Adopted Basis Newton-Raphson (ABNR) minimization, until the root mean square gradient was less than 0.001 kcal/mol Å. Docking was first carried out with Flo+ suite of programs.[49] The α_{1d}-AR and WB 4101 receptor complex was first submitted to 100 steps of flexible dynamic docking (DYNDOCK), with each step 300 ps long. The residues within 15 Å from the negatively charged oxygen atom of Asp176 were restrained in their original position, and a harmonic distance constraint between the same oxygen and the positively charged nitrogen atom of WB 4101 was imposed. In each run the temperature was cooled down from 600 to 300 K and the receptor structure then quenched. The unique conformations, according to a RMSD $\geqslant$0.5 calculated on the Cα atom trace, were stored and the best energy solution selected. Compounds **1**–**14** were further docked into the binding site carrying out fifty thousand runs of stochastic Monte Carlo docking (MCDOCK) with the whole binding kept fixed. The energy window for the selected agonists poses did not exceeded 3.3 kcal/mol above the best energy solution. GRINDs were calculated in GRID using the DRY, O, N1, and TIP atom probes to give four auto-correlograms and six cross-correlograms. PCA and PLS analyses were performed using the ALMOND software (version 3.3.0) using default settings. No initial scaling was applied to the original X-variable matrix which was subsequently filtered by three Fractional Factorial Design runs. Cross-validation was performed using the leave one out (LOO) procedure to select the optimal number of components in the PLS model equal to a significant increase of the cross-validation coefficient q^2 (at least 5%).

Acknowledgments

We thank the MIUR (Rome) and the University of Bari and Camerino for financial support. This study was also supported by Telethon-Italy (S00068TELU to F.F.).

Supplementary data

Supplementary data associated with this article can be found, in the online version, at doi:10.1016/j.bmc.2010.08.002.

References and notes

1. For part 9: Quaglia, W.; Piergentili, A.; Del Bello, F.; Farande, Y.; Giannella, M.; Pigini, M.; Rafaiani, G.; Carrieri, A.; Amantini, C.; Lucciarini, R.; Santoni, G.; Poggesi, E.; Leonardi, A. *J. Med. Chem.* **2008**, *51*, 6359.
2. http://www.pdb.org.
3. White, S. H. *Nature* **2009**, *459*, 344.
4. Palczewski, K.; Kumasaka, T.; Hori, T.; Behnke, C. A.; Motoshima, H.; Fox, B. A.; Le Trong, I.; Teller, D. C.; Okada, T.; Stenkamp, R. E.; Yamamoto, M.; Miyano, M. *Science* **2000**, *289*, 739.
5. Warne, T.; Serrano-Vega, M. J.; Baker, J. G.; Moukhametzianov, R.; Edwards, P. C.; Henderson, R.; Leslie, A. G. W.; Tate, C. G.; Schertler, G. F. X. *Nature* **2008**, *454*, 486.
6. Cherezov, V.; Rosenbaum, D. M.; Hanson, M. A.; Rasmussen, S. G. F.; Thian, F. S.; Kobilka, T. S.; Choi, H.-J.; Kuhn, P.; Weis, W. I.; Kobilka, B. K.; Stevens, R. C. *Science* **2007**, *318*, 1258.
7. Jaakola, V.-P.; Griffith, M. T.; Hanson, M. A.; Cherezov, V.; Chien, E. Y. T.; Lane, J. R.; Ijzerman, A. P.; Stevens, R. C. *Science* **2008**, *322*, 1211.
8. Fanelli, F.; De Benedetti, P. In *Antitargets*; Vaz, R. J., Klabunde, T., Eds.; Wiley-VCH, 2008; p 155.
9. Zhong, H.; Minneman, K. P. *Eur. J. Pharmacol.* **1999**, *375*, 261.
10. Price, D. T.; Lefkowitz, R. J.; Caron, M. G.; Berkowitz, D.; Schwinn, D. A. *Mol. Pharmacol.* **1994**, *45*, 171.
11. Michel, M. C. *Eur. Urol. Suppl.* **2002**, *1*, 5.
12. Roehrborn, C. G.; Schwinn, D. A. *J. Urol.* **2004**, *171*, 1029.
13. Romics, I. *Neurochem. Int.* **2007**, *51*, 328.

14. Chiu, G.; Li, S.; Connolly, P. J.; Pulito, V.; Liu, J.; Middleton, S. A. *Bioorg. Med. Chem. Lett.* **2007**, *17*, 3930.
15. Drouin, C.; Darracq, L.; Trovero, F.; Blanc, G.; Glowinski, J.; Cotecchia, S.; Tassin, J. P. *J. Neurosci.* **2002**, *22*, 2873.
16. McVary, K. T.; McKenna, K. E.; Lee, C. *Prostate Suppl.* **1998**, *8*, 2.
17. Quaglia, W.; Santoni, G.; Pigini, M.; Piergentili, A.; Gentili, F.; Buccioni, M.; Mosca, M.; Lucciarini, R.; Amantini, C.; Nabissi, M. I.; Ballarini, P.; Poggesi, E.; Leonardi, A.; Giannella, M. *J. Med. Chem.* **2005**, *48*, 7750.
18. Ballesteros, A.; Weinstein, H. *Methods Neurosci.* **1995**, *25*, 366.
19. Waugh, D. J. J.; Gaivin, R. J.; Zuscik, M. J.; Gonzalez-Cabrera, P.; Ross, S. A.; Yun, J.; Perez, D. M. *J. Biol. Chem.* **2001**, *276*, 25366.
20. Rosini, M.; Bolognesi, M. L.; Giardinà, D.; Minarini, A.; Tumiatti, V.; Melchiorre, C. *Curr. Top. Med. Chem.* **2007**, *7*, 147.
21. Quaglia, W.; Pigini, M.; Piergentili, A.; Giannella, M.; Marucci, G.; Poggesi, E.; Leonardi, A.; Melchiorre, C. *J. Med. Chem.* **1999**, *42*, 2961.
22. Wada, M.; Natsume, S.; Suzuki, S.; Uo, A.; Nakamura, M.; Hayase, S.; Erabi, T. *J. Organomet. Chem.* **1997**, *548*, 223.
23. Gardner, P. D.; Horton, W. J.; Pincock, R. E. *J. Am. Chem. Soc.* **1956**, *78*, 2541, and reference therein.
24. Pallavicini, M.; Fumagalli, L.; Gobbi, M.; Bolchi, C.; Colleoni, S.; Moroni, B.; Pedretti, A.; Rusconi, C.; Vistoli, G.; Valoti, E. *Eur. J. Med. Chem.* **2006**, *41*, 1025.
25. Bestmann, H. J.; Schulz, H.; Kunstmann, R.; Rostock, K. *Chem. Ber.* **1966**, *99*, 1906.
26. Berti, G.; Saettone, M. F. *Il Farmaco Ed Sci.* **1960**, *15*, 431.
27. Chen, X.; Green, B. E.; Kempf, D. J.; Li, L.; Norbeck, D. W.; Sham, H. L. Patent US 5905068 A, 1999; Chem. Abstr. 1999, 130, 352501.
28. Donnelly, A. C.; Mays, J. R.; Burlison, J. A.; Nelson, J. T.; Vielhauer, G.; Holzbeierlein, J.; Blagg, B. S. J. *J. Org. Chem.* **2008**, *73*, 8901.
29. Testa, R.; Taddei, C.; Poggesi, E.; Destefani, C.; Cotecchia, S.; Hieble, J. P.; Sulpizio, A. C.; Naselsky, D.; Bergsma, D.; Ellis, S.; Swift, A.; Ganguly, S.; Ruffolo, R. R.; Leonardi, A. *Pharmacol. Commun.* **1995**, *6*, 79.
30. Fargin, A.; Raymond, J. R.; Regan, J. W.; Cotecchia, S.; Lefkowitz, R. J.; Caron, M. G. *J. Biol. Chem.* **1989**, *264*, 14848.
31. Fargin, A.; Raymond, J. R.; Lohse, M. J.; Kobilka, B. K.; Caron, M. G.; Lefkowitz, R. J. *Nature* **1988**, *335*, 358.
32. Eltze, M.; Boer, R.; Sanders, K. H.; Kolassa, N. *Eur. J. Pharmacol.* **1991**, *202*, 33.
33. Ko, F. N.; Guh, J. H.; Yu, S. M.; Hou, Y. S.; Wu, Y. C.; Teng, C. M. *Br. J. Pharmacol.* **1994**, *112*, 1174.
34. Buckner, S. A.; Oheim, K. W.; Morse, P. A.; Knepper, S. M.; Hancock, A. A. *Eur. J. Pharmacol.* **1996**, *297*, 241.
35. Scapecchi, S.; Nesi, M.; Matucci, R.; Bellucci, C.; Buccioni, M.; Dei, S.; Guandalini, L.; Manetti, D.; Martini, E.; Marucci, G.; Romanelli, M. N.; Teodori, E.; Cirilli, R. *J. Med. Chem.* **2008**, *51*, 3905, and references therein.
36. QikProp, version 3.3, Schrödinger, LLC, New York, NY, 2010.
37. Fumagalli, L.; Bolchi, C.; Colleoni, S.; Gobbi, M.; Moroni, B.; Pallavicini, M.; Pedretti, A.; Villa, L.; Vistoli, G.; Valoti, E. *Bioorg. Med. Chem.* **2005**, *13*, 2547.
38. Strike, version 1.9, Schrödinger, LLC, New York, NY, 2010.
39. Quaglia, W.; Pigini, M.; Piergentili, A.; Giannella, M.; Gentili, F.; Marucci, G.; Carrieri, A.; Carotti, A.; Poggesi, E.; Leonardi, A.; Melchiorre, C. *J. Med. Chem.* **2002**, *45*, 1633.
40. Ballesteros, J. A.; Jensen, A. D.; Liapakis, G.; Rasmussen, S. G. F.; Shi, L.; Gether, U.; Javitch, J. A. *J. Biol. Chem.* **2001**, *276*, 29171.
41. Shi, L.; Liapakis, G.; Xu, R.; Guarnieri, F.; Ballesteros, J. A.; Javitch, J. A. *J. Biol. Chem.* **2002**, *277*, 40989.
42. Greasley, P. J.; Fanelli, F.; Rossier, O.; Abuin, L.; Cotecchia, S. *Mol. Pharmacol.* **2002**, *61*, 1025; reviewed in Fanelli, F.; De Benedetti, P. G. *Chem. Rev.* **2005**, *105*, 3297.
43. Topiol, S.; Sabio, M. *Biochem. Pharmacol.* **2009**, *78*, 11, and references therein.
44. Zhao, M. M.; Hwa, J.; Perez, D. M. *Mol. Pharmacol.* **1996**, *50*, 1118.
45. Pastor, M.; Cruciani, G.; McLay, I.; Pickett, S.; Clementi, S. *J. Med. Chem.* **2000**, *43*, 3233.
46. van Rossum, J. M. *Arch. Int. Pharmacodyn. Ther.* **1963**, *143*, 299.
47. De Lean, A.; Munson, P. J.; Rodbard, D. *Am. J. Physiol.* **1978**, *235*, E97.
48. Cheng, Y. C.; Prusoff, W. H. *Biochem. Pharmacol.* **1973**, *22*, 3099.
49. McMartin, C.; Bohacek, R. S. *J. Comput. Aided Mol. Des.* **1997**, *11*, 333.
50. Sali, A.; Blundell, T. L. *J. Mol. Biol.* **1993**, *234*, 779.
51. Im, W.; Feig, M.; Brooks, C. L., III *Biophys. J.* **2003**, *85*, 2900.